Hindawi
Adsorption Science & Technology
Volume 2022, Article ID 7998069, 16 pages
https://doi.org/10.1155/2022/7998069

Research Article

A Statistical Modeling and Optimization for Cr(VI) Adsorption from Aqueous Media via Teff Straw-Based Activated Carbon: Isotherm, Kinetics, and Thermodynamic Studies

Surafel Mustefa Beyan,[1] **Sundramurthy Venkatesa Prabhu**,[2] **Temesgen Abeto Ambio**,[1] **and C. Gomadurai**[3]

[1]*School of Chemical Engineering, Jimma Institute of Technology, Jimma University, Jimma, Oromia, Ethiopia*
[2]*Center of Excellence for Bioprocess and Biotechnology, Department of Chemical Engineering, College of Biological and Chemical Engineering, Addis Ababa Science and Technology University, Addis Ababa, Ethiopia*
[3]*Department of Chemical Engineering, Kongu Engineering College, Perundurai, Erode, Tamil Nadu 638060, India*

Correspondence should be addressed to Surafel Mustefa Beyan; surafel.beyan@ju.edu.et
and Sundramurthy Venkatesa Prabhu; haiitsvp@gmail.com

Received 23 September 2021; Revised 5 November 2021; Accepted 11 November 2021; Published 5 January 2022

Academic Editor: Amr Nassar

Currently, the growth of tannery industries causes a significant volume of waste disposal to the environment due to harmful Cr(VI). Long-time exposure to Cr(VI) imposes serious hazards on all living organisms. Hence, the treatment of tannery waste to remove Cr(VI) is not a choice but mandatory. Therefore, this study focused on the removal of Cr(VI) from the aqueous solutions via a teff (*Eragrostis tef*) straw based-activated carbon (TSAC) which was derived from locally available agricultural solid waste, teff straw (TS). The prepared TSAC was characterized using BET, FTIR, SEM, and XRD. A central composite approach-based RSM analysis was undertaken for statistical modeling and optimization for maximized Cr(VI) removal with respect to four important factors, namely, initial concentration of Cr(VI), the dosage of TSAC, pH, and adsorption time. Optimized values for maximizing adsorption of Cr(VI) (95% of removal) were acquired to be initial Cr(VI) concentration: 87.57 mg/L, TSAC dosage: 2.742 g/100 mL, pH: 2.2, and contact time:109 min. The results from the design of the experiment were also analyzed for the significance of the interaction between the selected process parameters. In addition, the pseudo-second-order kinetic and Langmuir isotherm models were found suitable for describing the adsorption data. The adsorption capacity of Cr(VI) on TSAC was 19.48 mg/g. The observed thermodynamic characteristics reveal that Cr(VI) adsorption on TASC is endothermic in nature. From the results, TSAC had shown a potential Cr(VI) efficiency on optimized process conditions that can be exploited effectively as adsorbent for removal of Cr(VI)-contaminated wastes.

1. Introduction

The rate of contaminated wastewater has kept on increasing intensively as a result of rapid urbanization and industrialization. According to the report by UNWWAP in 2017 [1], approximately 80% of wastewater is discharged to water sources without being properly treated. Due to several toxic contaminants and their harshness, the natural environment is getting affected. This issue should be concerned seriously specifically to third-world countries like Ethiopia since they dispose of approximately 90% of contaminated wastewater to the landfill without being treated properly [1, 2]. Recently, the fast growth of industrialization causes a large amount of heavy metal-laden disposal to the environment which is highly toxic, mutagenic, and oncogenic. Among the different industries, leather industries release a significant volume of Cr(VI)-laden wastewater [3].

Tanning is one of the most important and critical processes in which durable leathers are formed. It produces fewer vulnerabilities to decompose [2]. This process

compromises different steps in strengthening the protein structure of rotten skin through tannins and peptide bond-making. During this processing, salt, enzymes, acids, and tanning agent are used to break down fat protein and nonfiler's structure.

At present, roughly 80% of leather industries practice chromium for the tanning process since its water can rattle down the surface successfully with appropriate retaining and plausible to attain rawhide with a firm color and high stability of thermal resistance, colloquially, known as chrome tanning. Chrome tanning uses salt solution corresponding to Cr(III) sulfate to tan hides. Following the utilization of Cr salt agents, the bath is salted by sodium bicarbonate aimed at intensifying the pH around 4 to 5 to activate cross-linking among the chromium and collagen. Since Cr can frame steady bridge bonds, it makes it the most utilized tanning agent.

During Cr tanning, about60% of Cr(III) is being utilized and the remains are just dumped in the sludge [2]. Sludge discarding on land is a longstanding technique, a common practice. Sun-drying and heat effects make the Cr(III) compounds oxidize to change into toxic Cr(VI), which is highly mutagenic and oncogenic [4]. In 2015 studied data by Black-Smith Institute [5], around 16 million people of the word have been affected by chromium-causing diseases. Chromium shows a hazardous effect on the aquatic's environment, such as in invertebrate animals, algae, fish, and aquatic plants. Toxicologists have proven that Cr(VI) even at low concentration exhibits growth reduction and reduction of photosynthesis rate in aquatic plants and algae, behavioral change, reduced reproduction, and growth in invertebrates' animal and fish survival ability [6].

Currently, there are about 35 leather industries in Ethiopia. Almost all of them are processing with chromium in the tanning. The generated chromium contained waste is discharged into the environment [7]. Cr maintains in transition metal oxides (Cr(II) to Cr(VI)) [2]. Usually, two of the most dangerous elements are Cr(III) and Cr(VI). Effluents from tanneries, fertilizers, pigment industries, sewage, oil well drilling, and fertilizer industries are main the sources. Due to Cr phytotoxicity, crops are affected by inhibition of seed germination, leaf chlorosis, deficiency in root growth, etc. [8]. Cr(VI) has been categorized as a category 1 carcinogen to humans, indicating the seriousness of the Cr(VI) risk [9]. Consequentially, it will lead to a hazardous effect on aquatic organisms and yet worsen the community that lives near the river drinks if the river water is contaminated by Cr(VI). Thus, they will be affected by different diseases such as cacogenics and others. Berihun studied the concentration content of discharged Cr(VI) in the environment in the Ethiopian leather industries. From his report, the concentration of Cr(VI) in the effluent is in the range of 26-47 mg/L [10]. However, according to the World Health Organization and Ethiopian environment protection authority standard, the concentration of Cr(VI) discharge to the environment is 0.1 mg/L [11]. As the health hazards either in aquatic life or human being are caused by Cr(VI), hence, appropriate treatment to get rid of excessive Cr is not a choice but mandatory.

For keeping environmental concerns, to get rid of different living organism threats, cause because of this tannery mud disposal, it is critical to give dip vital for Cr(VI) disposal from the tannery sludge. However, different treatments are accessible to get rid of the toxins from the sludge with their limitations; for instance, the process is not economical and has small detoxification effectiveness even though they are having been broadly put into practice; it is not only these practices that suffer from numerous limitations together with low selectivity, metal removal, requiring high amount of reagent, and energy consumption and also generates secondary wastes that are problematic to dispose of [12, 13]. Anyway, the adsorption process using low-cost adsorbents with high efficient heavy metal removal still gains huge interest among researchers. It shows efficient outcome and is simple and economical; in developing countries like Ethiopia, low-cost adsorbent-based waste treatment process gains huge value. In this way, activated carbon (AC) is the most extensively utilized adsorbent owing to its high porosity. It can be used for adsorbing heavy metals. However, commercially accessible activated carbons are very expensive; thus, researchers are keeping their research to look for different biomaterial-based activated carbon that can be affordable.

Teff (*Eragrostis tef*) straw (TS) is an abundant and native lignocellulosic material in Ethiopia and found as a residual waste after seeds were removed from the teff plant (Eragrostis teff) [14]. Globally, Ethiopia harvests teff plant in the largest quantity, and it accounts for approximately 25% of all harvested crop products in 2017 [14]. After the seed of the teff is removed from the plant, the straw is discarded as agricultural waste.

Hence, the teff straw could be a potential source material for preparing activated carbon. So far, there is no appreciable information on adsorption studies using teff straw-based activated carbon (TSAC). Also, there are very limited studies carried out on heavy metal removal using TSAC. Keeping this view, the current study has emphasized using the teff straw-based activated carbon prepared from teff straw for removing hexavalent chromium from an aqueous synthetic media.

Different reviews of investigations with respect to teff straw-based activated carbon showed that bioadsorbent efficiency to absorb heavy metal is predominately influenced by several factors, such as contact time, initial pH, adsorbent dosage, sludge loading, and concentration of toxic element [13, 15, 16].

The response surface approach (RSM) practices scientific means to found the interrelation among arithmetical input parameters for defining optimal points and treatment of wastewater practice [17]. By using RSM in adsorption technology using teff straw-based activated carbon, a smaller number of experimental setups are essential and also saving time and involvement expense giving more reliable results.

Up to the present, comprehensive research has not been done on RSM grounded optimization and removal of hexavalent chromium as of tannery effluent using teff straw-based activated carbon in batch mode adsorption. Thus, this study is the first to report on RSM-based optimization of

hexavalent chromium by teff straw-based activated carbon from tannery effluent and support the data while doing isotherm and kinetic model for the removal process. Further, characterizations of the obtained teff straw activated carbon were carried out.

2. Material and Method

2.1. Materials and Chemicals. Reagents and chemicals that have been utilized in this research were graded analytical and have purity greater than 98%. They were gotten from Sigma-Aldrich. Teff straw (TS) was a solid waste obtained from teff, and it is collected in Addis Ababa, Ethiopia, from farmland.

One gram per liter of aqueous Cr(VI) solution was ready through liquifying in $K_2Cr_2O_7$ in ultrapurified water. Further, it was diluted to appropriate concentrations. The test pH solution was accustomed by the addition of drops of either HCl or NaOH (1 mol/L) whenever vital. An Atomic Absorption Spectrometer (PerkinElmer, Model-PINAACLE 900T) was employed in order to measure the Cr(VI) concentration via adopting the standard procedure.

2.2. Preparation of TS-Based AC. Teff straw was cleaned with water numerous times to get rid of the dirt from it and subsequently put into the oven at 105°C for one day in order to take away the moisture. Then, the TS was pulverized by an electric grinding motor and it was sieved to a particle size of 250 μm, and it was once more cleaned several times by water that is purified via reverse osmosis process. Finally, it was put into the oven at 105°C overnight before it was chemically impregnated and thermally treated. So as to activate the mixture 1 : 3 (w/$w$ratio), TS particle with sulfuric acid (concentrated) was prepared. The H_2SO_4 was used as a desiccating agent which detains the assembly of tar; hence, activated carbon would have refined porosity. Chemically activated TS materials were put into the oven for 2 hr at 110°C. Finally, it was carbonized at 450°C in a muffle furnace. Then, the teff straw-based activated carbon (TSAC) obtained from the muffle furnace was pulverized and separated to a magnitude of 250 μm and 300 μm. The TSAC was cleaned with water that was distilled numerous times, and it was soaked in the distilled water for the night in order to reach neutral pH. Again, the particle was sieved to the size of 250 μm, and it was kept in a vacuum desiccator until it was used for the adsorption study.

2.3. Characterizations of TSAC. The teff straw-based activated carbon samples (TSAC) were analyzed regarding its physicochemical properties. American Standard Test Method (ASTM international) standard procedure was employed in order to analyze the TSAC as presented in Table 1.

BET- (Brunauer–Emmett–Teller; SA-9600, USA) specific surface area was gotten by melting point examination of inert nitrogen gas through one-track layer adsorption on the surface of TSAC at the temperature of -196.15°C. An inert gas of helium at a pressure of 2 MPa was employed as a transporter for the inert nitrogen gas (2.5 MPa) and to remove air into the atmosphere. A combination of inert nitrogen and helium gas at 20%, 30%, and 50% was accustomed to measure the specific surface area. 0.1 g of pretreated TSAC was prepared at a temperature of 120°C for 1 hr.

Table 1: Standard procedures accustomed in order to quantify physiochemical characteristics.

TSAC characterization	Used standard methods	References
Moisture content determination	ASTM D2495-07	[18]
Ash content determination	ASTM D2866-11	[19]
Volatile matter content determination	ASTM D5832-98	[20]
Bulk density determination	ASTM D2854-09	[21]
Fixed carbon determination	ASTM D7582-15 2015	[22]
Carbon yield		[23]
Point zero charge		[24]
pH	ASTM E70-19	[25]

In order to recognize the morphological surface of TSAC, SEM (scanning electron microscope; FEI, INSPCT-F50, Germany) analysis was performed. The adsorbent was positioned on stubs of aluminum, enclosed by means of a carbon conductive glue tape, and pictured through SEM images, operated at 15.00 kV, 50 μm working space under a vacuum.

TSAC was explored using FTIR (Fourier transform infrared spectroscopy; iS50 ABX, Germany) in the spectral region range of 400 $cm^{-1}$to 4000 cm^{-1} to find out its functional groups. These spectrums are produced by using infrared light as a source, and the KBr pellet method was employed to achieve FTIR characterization of the sample.

In addition, XRD (Olympus BTX-528 XRD) investigation was done on TSAC in order to examine the amorphous and crystallinity nature of the sample. The XRD study was studied by Cu-Co with an energy source occupied on a 40 kV power voltage and 25 mA current. The X-ray diffraction was carried out between the 2θ angle range, 10° to 70°. Four was a split threshold value.

2.4. Adsorption Capacity. The prepared AC adsorption activity can be evaluated by the capacity of adsorption determination. At conditions of equilibrium, capacity of adsorption was determined via equation (1). For determining the adsorption capacity, a solution of 25 mL volume containing the concentration of 50 mg/L Cr(VI) with prepared adsorbent had been taken. The dosage of adsorbent was taken as 0.05 g. The adsorption reaction was carried out with the stirring speed of 400 rpm for 2 h.

$$Q\,(\mathrm{mg/g}) = \frac{(C_1 - C_2)V}{M}, \tag{1}$$

where Q is nothing but sorption capacity, C_1 refers to the initial concentration of Cr(VI) ions (mg/L), C_2 refers to the concentration of Cr(VI) ions at equilibrium (mg/L), V is the volume (L), and M is the weight of the adsorbent (g).

2.5. Batch Adsorption Experiment for Cr(VI) Removal Using CCD Statistical Tool. One variable at a time method was employed in order to resolve the average levels of selected variables that are very important aimed at employing design of experiment (DOE). Adsorption by batch base tests was carried out in order to examine the consequence of initial hexavalent chromium concentration (Cr(VI)), pH, contact me, and TSAC quantity on Cr(VI) adsorption efficacy of TSAC.

A conical beaker containing 0.1 L of the sample was mixed via a thermostatic mover and shaker at room temperature and 200 rpm for each experiment runs. Next, the solution was sieved via means of filter paper (Whatman No. 1), and the clear liquid was investigated for concentration of residue Cr(VI) ion by the AAS tool, and for each sample analysis, a blank solution was measured. Next, the adsorption efficiency of TSAC was carried out (equation (2)) [13]. The one-variable experiment results were very consistent with different researches [26–28] (Table S1).

$$\text{Removal efficiency}\,(\%) = \frac{C_o - C_t}{C_o} \times 100, \tag{2}$$

where C_o (mg/L) and C_t(mg/L) refer to the initial concentrations of Cr(VI) and concentration at a required time t, respectively.

Experiments were carried out to optimize the selected parameters for improving the adsorption efficiency of TSAC and examine the collaboration effects of TSAC dosage, contact time, pH, and hexavalent chromium on the adsorption effectiveness of Cr(VI) from the synthetic solution via TSAC. Other influencing parameters (agitation speed: 200 rpm at room temperature) were fixed as constant. For RSM investigation, the grouping of the chosen variables was engaged employing the central composite design (CCD) approach. It warrants that each factor and the effects of their relationships are methodically investigated. The selected variables and their corresponding level are tabulated in Table 2. Grounding on the figure of constraints, CCD proposed a grouping of thirty experiments that justifies axial, factorial, and average levels. Thus, each experimentation was studied in triplicate and the mean value of obtained results was recorded. The obtained remarks found from the CCD experiments were statistically investigated and fitted to a polynomial equation model for developing an empirical mathematical equation that can express the association among the response of the experiment and parameters. The polynomial equation (3) is described as.

$$R = \theta_0 + \sum_{j=1}^{4} \theta_j Y_j + \sum_{j=1}^{4} \theta_{jj} Y_j^2 + \sum_{i} \sum_{<j=2}^{4} \theta_{ji} Y_i Y_j + e_i, \tag{3}$$

where R is the response (Cr(VI) removal (%)); Y_i and Y_j refer to variables (i and j range from 1 to k); θ_0 refer to the coefficient of intercept; θ_j, θ_{jj}, and θ_{ij} are known to be coefficients of interaction for the variables, respectively; and e_i is known as error.

Additionally, the process variables were optimized for the goal of maximizing the Cr(VI) removal using mathematical optimization. Evaluations of all statistical constraints were achieved by means of ANOVA (analysis of variance). Through solving the equation regression of the chosen variables, the optimal values were found. The effects of interactions between the factors were investigated by conducting a response surface plot. RSM and CCD investigations were developed with help of Design-Expert 12. The verification of the developed model, predicted by the design expert, was proven through performing a triplicate experimental run.

2.6. Isotherm and Kinetic Studies on Cr(VI) Removal. For isotherm and kinetic studies, different initial concentrations of hexavalent chromium, that is, 40, 80, 120, 160, 200, and 240 mg/L, with the optimal values of pH, TSAC dosage, and contact time which are obtained from statistical equation of RSM modeling were used. The equilibrium metal ion concentration (C_e), the adsorption capacity at q_e at equilibrium condition, and the specific adsorption (C_e/q_e) were determined in order to evaluate the adsorption isotherm. The observed data were investigated for the appropriateness of isotherms by fitting it to the model of equation. In this study, Langmuir (plot of C_e/q_e vs. C_e) (equation (12)) and Freundlich (plot of log q_e vs. 1/log C_e) (equation (13)) isotherms were evaluated using the values of R^2.

The kinetics of Cr(VI) adsorption was investigated through batch mode adsorption method, that is, by sating Cr(VI) concentration, TSAC quantity, and pH at their optimal level and with the various times of contact (20, 40, 60, 80, 100, 120, and 140 min). Next, the adsorption kinetics were gotten by finding out the quantity of adsorbate adsorbed at a q_e and adsorbed adsorbate at any instantaneous time t (q_t). Further, the adsorption experimental data were examined for the appropriate fitness to the different kinetic models such as pseudofirst order (plot of log $(q_e - q_t)$ vs. t) (equation (15)) and pseudosecond order (plot of $1/q_t$ vs. t) (equation (16)).

The intraparticle diffusion kinetic model was considered to analyze using Weber-Morris plot. It can be generated by q_t vs. $t^{1/2}$ (Figure 1), while the t is contact time. k_w is known as intraparticle diffusion rate constant (equation (4)). The use of this kinetic study can provide an idea of boundary layer thickness. This is accredited to the instant use of the readily accessible absorbing spots on the adsorbent surface. The parameters, k_w and C, were deduced from the slope and intercept of the linear equation of the Weber-Morris plot. The Elovich model of equation is an interesting model that can describe about the activated chemisorption (Figure 2). In this model, a_e and b_e are known to be constants that represent as initial sorption rate and extent of the surface coverage, respectively (equation (5)). In addition, Bangham's model was used to know about the slow step occurring in the TSAC adsorption system, where C_0 refers to the initial concentration of Cr(VI) in the solution. V refers to the volume of the solution, and m is the weight of the adsorbent used per liter of solution. The value of parameters for k_B and α was determined from the linear plot of log

Table 2: Levels of the four studied independent parameters.

Parameters	Parameter coding	Unit	-1 (low level)	-1 (high level)	-α	+α
Initial Cr(VI) concentration	A	Mg/L	60	140	20	180
TSAC dosage	B	g/100 mL	2	4	1	5
pH	C	—	2	3	1.5	3.5
Contact time	D	Min	60	120	30	150

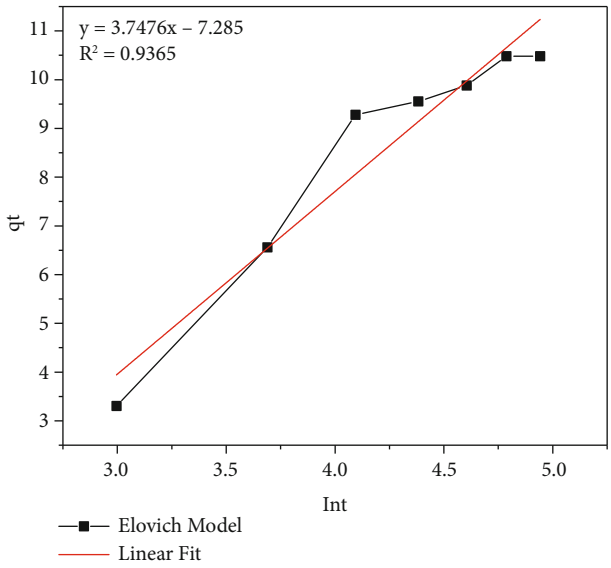

Figure 1: The plot generated using the Elovich model for the removal of Cr(VI) by TSAC.

$\{\log [(C_0/(C_0 - q_t m)]\}$ versus $[\log t]$ (Figure 3) using the slope and intercept (equation (6)).

$$q_t = k_w t^{1/2} + C, \tag{4}$$

$$q_t = \left[\frac{\ln (a_e b_e)}{b_e}\right] + \left(\frac{1}{b_e}\right) \ln t, \tag{5}$$

$$\log \log \left[\frac{C_o}{(C_o - q_t m)}\right] = \log \left(\frac{k_b m}{2.303 V}\right) + \alpha \log t. \tag{6}$$

2.7. Thermodynamic Studies on Adsorption. To investigate the thermodynamic performance of biosorption process for Cr(VI) on the TSAC, the thermodynamic parameters such as free energy change (ΔG^0), enthalpy change (ΔH^0), and entropy change (ΔS^0) were determined using equations (7) and (8), respectively.

$$\Delta G^o = -RT \ln K_a, \tag{7}$$

$$\ln K_a = \frac{\Delta H^o}{RT} + \frac{\Delta S^o}{R}, \tag{8}$$

where R refers to the universal gas constant ($R = 8.314$ J/mol K), K_d refers to the distribution coefficient ($K_d = q_e/C_e$) (L/g), and T refers to absolute temperature (K). Using the relation (xxx), ΔG^0 was calculated at different temperatures such as 25, 40, and 60°C. Equation (8) is known as Van't Hoff Eq which can be used to determine the values of ΔS and ΔH.

2.8. Studies on Desorption and Regeneration of Adsorbent. The reusability of the bioadsorbent can be examined by desorption test. In order to explore the reverse activity for chromium adsorption by TSAC, the batch desorption studies were carried out. For the desorption studies, different concentrations of HNO_3 and HCl solutions 1-10 (mol/L) were considered to perform the regeneration process. For this, 2 g of air-dried TSAC which was loaded with Cr(VI) was used. Chromium-loaded bioadsorbent was transferred to 250 mL flasks containing 100 mL of desorbing eluents (HNO_3 and HCl). The solutions were constantly agitated in an orbital shaker at 100 rpm with 30°C (Biosan, Orbital Shaking Incubator, ES-20). The desorption processes were carried out for both acids which did not exceed for 2 h. The desorption efficiency (%) of Cr(VI) from the solid phase of TSAC was calculated as

$$\text{Desorption efficacy } (\%) = \frac{C_1}{C_2} \times 100\%, \tag{9}$$

where C_1 refers to the amount of Cr(VI) released into the aqueous solution and C_2 refers to the amount of Cr(VI) adsorbed by the biosorbent (mg/L), respectively.

3. Results and Discussions

3.1. Characterization of TSAC. The physicochemical feature of a TSAC was investigated by the American Standard Test Method (ASTM), and the data had been tabulated as shown in Table 3. Moisture content (MC) determinations state the amount of substance vaporized mainly water. Lower VM, MC, and AC of teff straw activated carbon signposted as it can be vastly porous material and contains fewer hydrophobic and noncarbon components in its nature [11]. The characteristics of properties that have been presented in Table 3 showed a lower value of MC, AC, and VM and a high percentage of FCC demonstrating a high graphitization grade and a low number of functional groups. The high FCC and CY of TSAC were too sympathetic for the practicability of the synthesis of TSAC adsorbent [29]. The FCC and CY of TSAC are also importantly larger than those detected for other lignocellulose sources of precursors, for instance, corncob and coffee husk-based ACs [13, 30]. For the possible use of AC, the density of bulk should not be lower than 0.25 g/cm^3. As presented in the table, the TSAC has a bulk density of 0.79 g/cm^3 and this result satisfies the above condition. The charged chromium hexavalent of group adsorption onto the surface of

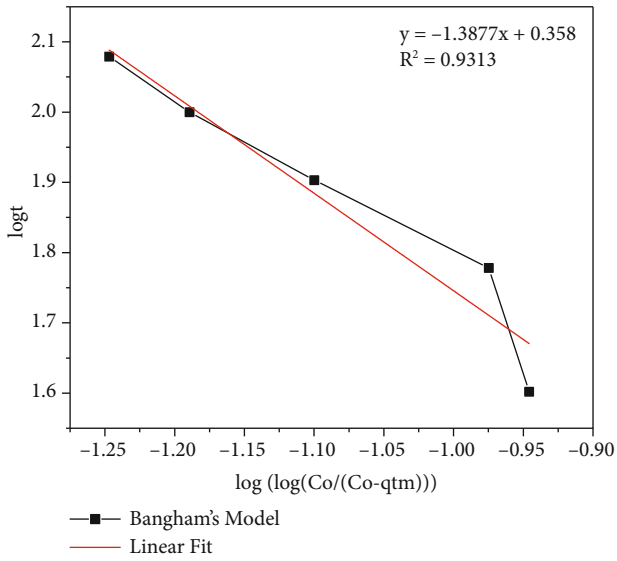

FIGURE 2: The plot generated using Bangham's model for the removal of Cr(VI) by TSAC.

TSAC is principally influenced by the adsorbent surface charge, which is in turn impacted by the pH of the solution. The association between P_{ZC} and capacity of adsorbent (TSAC) is that adsorption of cations on whichever adsorbent will be likely to upsurge at P_{ZC} value lower than pH value while anion adsorption will be advantageous at P_{ZC} values greater than the value of the pH [31].

The specific surface area of prepared TSAC was observed to be 456 m^2/g according to analysis of the BET. This result confirmed that the concentrated H_2SO_4 formed porosity on the teff straw and made it a TSAC. Nevertheless, the obtained BET-specific surface area of TSAC is relatively lesser than commercially obtainable AC [12]. This result is also supported by the SEM morphology of the TSAC (Figure 4).

SEM has been a fundamental tool for defining the morphology of the surface and to have insight into the physical properties and structure of the adsorbent. Figure 4 presents the SEM image of the synthesized TSAC, and the surface morphology looks as if canal resembles the pore surface structure of the adsorbent, and this surface porosity could be well thought out as a factor for heavy metal, Cr(VI), binding.

FTIR methods (Figure 5) have been used to establish the identity of the important functional group that is found in the TSAC adsorbent. The broad peak at about 3397 cm^{-1} could be designated to the -OH stretching vibration mode of hydroxyl functional compound, and this is due to the existence of cellulose. The existence of a small band located at 2823.41 cm^{-1} is assigned to C–H vibrational stretching of the methylene and methyl group [17]. The peak located around 1628 cm^{-1} corresponds to an aromatic carbon (stretch of C=C in pungent ring) and carboxyl group (C=O stretch). The small peak at 1316.04 cm^{-1} can be credited to O–H and C–O stretching vibration modes [32, 33]. The sharp shoulder at around 1035 cm^{-1} could be the consequence of ionized connection P^+-O^- in acidic phosphates to the symmetric quivering of the C–O–P chain [13].

$$-C-OH + H_3PO_4 -- C-O-PO(OH)_2 + H_2O \quad (10)$$

The small peak at 518 cm^{-1} is ascribed to P–C phosphorous containing the compound. From the FITR analysis, it is understandable that H_3PO_4 activation upsurges the oxygen-containing functional groups, such as phosphate groups and hydroxyl of the acidic and phenolic compound on the carbon surface of the adsorbent. Thus, Cr(VI) adsorption is most likely occurring and this is mainly due to ion exchange, surface complexation through oxygen bonding, or van der Waals force.

For adsorption of Cr(VI), a comparison by FTIR was done before and after the adsorption process and the obtained result showed the differences in the peaks of the absorbance position. After the adsorption process, the broad peak at the position of 3397 cm^{-1} was distorted signifying that interactions of chemicals have happened among the hydroxyl group of the TSAC and the Cr(VI) ions. The intensity of the vibration at 2823.41 cm^{-1}, 1628 cm^{-1}, 1316.04 cm^{-1}, and 518 cm^{-1} was decreased and 1403 cm^{-1}, carboxylate ion stretching bond of C=O, appeared after the process of adsorption. These vicissitudes signposted aliphatic functional, namely, –CH2, CH3, and C=O and OH group involvement in adsorption of hexavalent chromium and complexation of surface occurrence. Previous results by different researchers support the findings of this study [34–37].

XRD is a measurement system that distinguishes statistics about the structure of the crystal, mineral composition, and material properties. As indicated by Figure 6, the large hill of the activated carbon, from 22.12° to 35.05° indicated the existence of amorphous compounds. The peak at 2θ of 36.88, 39.95, 41.58, and 60.60° demonstrates the existence of a crystalline structure. This crystalline structure existence is due to the chemical activation process of the teff straw. Similar results were found in the previously reported data by Beyan et al. [12]. The major crystalline minerals were found to be Mn_2Sb and Jagowerite.

3.2. Adsorption Capacity. The adsorption capacity of the TSAC was observed to be 19.48 mg/g which was comparatively better than the commercial activated carbon (17.63 mg/g) that was procured from Sigma-Aldrich (product code—161551).A brief summary of comparison for adsorption capacity has been shown in Table 4.

3.3. Batch Adsorption of Cr(VI) Using CCD of Experiment

3.3.1. Model Development for Cr(VI) Removal. Five points for each constraint of the process were chosen grounding on the uppermost removal efficacy from the batch mode of adsorption according to one variable at a time approach and different works of pieces of literature [26–28]. RSM-CCD method was employed in order to choose the effective model for the process and to improve the adsorption process parameters by optimization [33].

The effects of interactions for the four considered parameters, namely, initial Cr(VI) concentration (A), TSAC dose (B), solution pH (C), and contact time or adsorption period (D), on the removal efficiency of Cr(VI) were

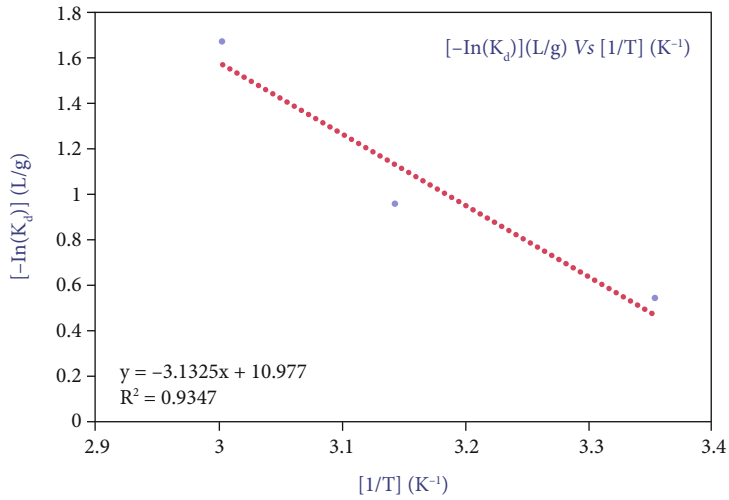

Figure 3: Fitting of adsorption data to the plot of ln (K_d) *vs.* $[1/T]$.

Table 3: Physiochemical characterization of activated carbons.

Activated carbon	Characteristics of activated carbon									
	pH	C(mS/cm)	MC (%)	AC (%)	VM (%)	FCC (%)	CY (%)	BD (g/cm^3)	SA m^2/gm	P_{ZC}
TSAC	7.05	0.59	6.13	5.34	19.42	69.11	59.4	0.79	456	4.89

C is conductivity, MC is moisture content, AC refers to the content of ash, VM is nothing but the volatile matter, FCC is fixed carbon content, CY is carbon yield, BD is bulk density, SA is surface area, and P_{ZC} is point zero charge.

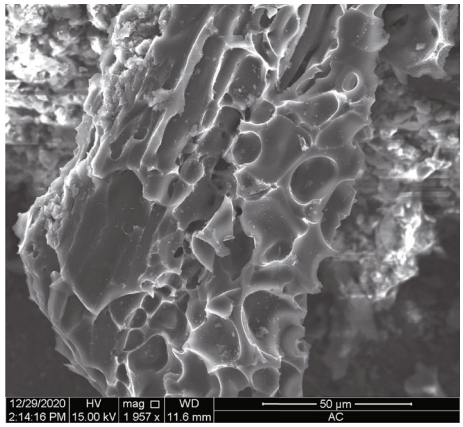

Figure 4: SEM image of activated carbon prepared from teff straw.

investigated with thirty arbitrary experimental trials that are obtained via the CCD method. The percentage removal efficiency of Cr(VI) from the samples via means of TSAC was obtained in the range of 71.31 to 96.56% (Table 5). The maximum residual between the actual experiment and the predicted one is only 2.5 which proves they are in close agreement.

Based on adjusted and predicted values of R^2 (0.9687 and 0.9293, respectively), the quadratic model was chosen which can be more appropriate for fitting the model to represent Cr(VI) adsorption efficacy by TSAC. Further, the prediction accomplishment using the quadratic model was implemented in the present study (equation (11)). This equation by coded factor has advantage of finding the comparative influence of the constraints by comparing the coefficients of the constraints [14]. The obtained results were observed to be reliable with the previously studied experiment on adsorption of Cr(VI) via various activated carbons prepared using different agricultural residues [42, 43]. The coded quadratic equation (11) presented clearly that except for the contact time, all other parameters have negative coefficient and this means after their optimum value, further addition of these parameters causes declination in the removal efficiency of Cr(VI) by TSAC.

$$\begin{aligned}\text{Cr (VI) removal (\%)} = {} & +94.04 - 3.25A - 1.37B - 2.07C \\ & + 2.66D - 1.11\text{AB} - 1.20AC \\ & - 0.4294AD + 0.2094BC \\ & - 0.9119BD - 1.21CD - 4.14A^2 \\ & - 3.35B^2 - 2.28C^2 - 2.83D^2.\end{aligned} \tag{11}$$

ANOVA assessment was executed to investigate the import of the individual process parameter and their combined interaction effect on the adsorption efficiency of TSAC to Cr(VI) metal. According to statistical analysis, the developed model was observed to be more significant [12]. This showed that most of the constraints are noteworthy; thus, these process variables are effective on removal of Cr(VI) via TSAC. This discovery is also in pact with various previous researches which are carried out on activated carbon prepared from agricultural wastes [42, 43]. For Cr(VI) removal percent, the model has a *p* value of less than 0.0001 and the *F*-value was 65.19 (Table S2). The lack of fit Cr(VI) removal was 0.5084 which is insignificant

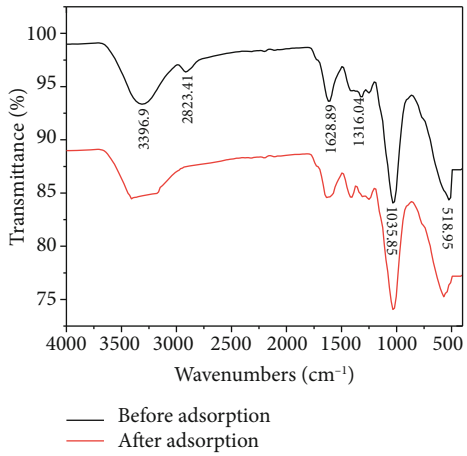

Figure 5: The FTIR spectra of teff straw-based activated carbon before and after the adsorption process.

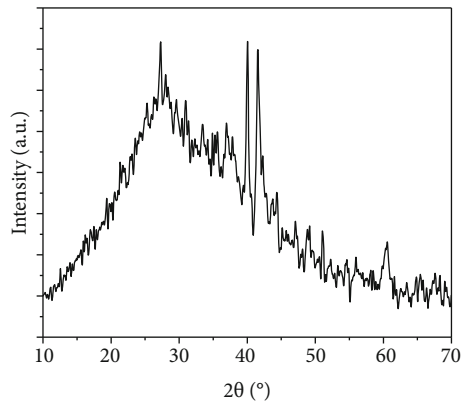

Figure 6: The XRD spectrum of teff straw-based activated carbon.

Table 4: Comparison of adsorption capacities of Cr(VI) on different adsorbents.

Adsorbent	Adsorption capacity (mg/g)	Reference
TSCA	19.48	Present work
Commercial activated carbon	17.63	Present work
ACAP	18.78	[38]
RSS	15.47	[39]
ATSAC	21.75	[40]
PSAC	16.26	[41]

relative to the pure error. Signal to noise ratio was determined via precision of Adeq, and its value was attained to be 25.65 which indicated a satisfactory signal of the quadratic equation for removal of Cr(VI) [44]. This ratio must be greater than four in order to signify the correctness of the second-order polynomial equation in predicting the response. Accordingly, this model for the removal of Cr(VI) can be evaluated for use in the navigation of design space. In addition, the coefficient of variation (CV = 1.52) would like to be reduced because a lower value supports the reliability with which the tests were carried out [2].

3.3.2. Interaction Effect Analysis of the Parameters. With the aid of the RSM-CCD method, the significance of the selected process parameters, namely, Cr(VI) initial concentration, TSAC dosage, pH, and adsorption period, was investigated on the adsorption effectiveness of Cr(VI). By putting the other process factors constant, the interaction effect of two factors on Cr(VI) removal was examined and given as below utilizing 3D response surface schemes (Figure 7).

The interaction outcomes of initial Cr(VI) concentration and TSAC dosage are shown in Figure 7(a). From the plot of 3D, it is clearly understood that removal percentage increases as the concentration of initial Cr(VI) decreases from 180 to 90 mg/L and also rises in TSAC dose from 2 g/100 mL to 3 g/100 mL. As it is given from the response variable coded equation, the mutual interaction relation of Cr(VI) initial concentration and TSAC dosage has a nondesirable effect on the adsorption efficiency with the coefficient of -1.1 (equation (11)). As given in Table S2, it has a substantial effect with a p value less than 0.0033 too. The peak for removal efficiency was gotten at 100 mg/L and 3 g/100 mL of initial concentration of Cr(VI) and TSAC dosage, respectively.

Figure 7(b) explains the 3D plot of the combined relations of initial concentration of Cr(VI) and a solution pH at the mean of contact time and TSAC dose. The removal efficacy was enlarged with the decreasing the pH of the solution and obtaining the highest removal effectiveness of the adsorbent at a pH of 2.5. It can also be understood that the adsorbent efficiency upsurges with the reduction of initial Cr(VI) concentration. With the coefficient of –1.2 (equation (11)), the removal efficiency is affected by the collective effect of initial Cr(VI) concentration and solution pH. The interaction effect has a significant effect on its Cr(VI) adsorption via TSAC with the p value of 0.0019.

The interaction of the combined effect on the initial concentration of Cr(VI) and adsorption time on TSAC adsorption efficacy is plotted in Figure 7(c). The 3D plots showed clearly that as the time for contact increases from 60 min to 90 min, the removal efficiency gets increased and got constant as increased beyond 90 min. The combined interaction effect of contact time and Cr(VI) initial concentration affects the removal efficiency undesirably by a coefficient of –0.4294 (equation (11)). The highest adsorption of hexavalent chromium is gotten at a contact time of 90 and an initial Cr(VI) concentration of 100 mg/L.

The combined effect of TSAC dose and pH of the solution on the removal efficiency is given in Figure 7(d). The proficiency of removal became upsurge with the decrease in pH until it reaches 2.5, and it is increased with TSAC dose increments (3 g/100 mL), but it goes downward with further addition of TSAC. As observed from the response of quadratic equation (equation (11)), the interaction effect of TSAC dose and solution pH has a positive effect on the removal efficiency with a coefficient of +0.2094. The removal efficiency of Cr(VI) was attained at a TSAC dose of 3 g/100 mL and a pH of 2.5.

Table 5: Independent parameters of CCD matrix used in RSM with the equivalent experimental and predicted values for response.

Standard order	Run order	Actual variables				Removal efficiency of Cr(VI) (%)	
		A	*B*	*C*	*D*	Experimental	Predicted
24	1	100	3	2.5	150	90.06	88.01
7	2	60	4	3	60	83.25	82.78
2	3	140	2	2	60	79.67	79.79
12	4	140	4	2	120	80.25	81.25
4	5	140	4	2	60	76.67	76.67
30	6	100	3	2.5	90	93.65	94.04
18	7	180	3	2.5	90	71.31	70.96
22	8	100	3	3.5	90	81.28	80.79
9	9	60	2	2	120	90.54	91.22
28	10	100	3	2.5	90	96.56	94.04
14	11	140	2	3	120	78.14	79.11
5	12	60	2	3	60	80.76	81.06
15	13	60	4	3	120	83.51	84.72
16	14	140	4	3	120	73.12	72.75
21	15	100	3	1.5	90	90.21	89.08
29	16	100	3	2.5	90	93.24	94.04
25	17	100	3	2.5	90	93.75	94.04
19	18	100	1	2.5	90	84.45	83.35
13	19	60	2	3	120	85.91	86.35
6	20	140	2	3	60	75.65	75.24
8	21	140	4	3	60	71.89	72.53
27	22	100	3	2.5	90	93.45	94.04
20	23	100	5	2.5	90	78.41	77.88
23	24	100	3	2.5	30	76.96	77.39
10	25	140	2	2	120	87.71	88.48
11	26	60	4	2	120	87.76	88.46
17	27	20	3	2.5	90	85.23	83.96
26	28	100	3	2.5	90	93.56	94.04
3	29	60	4	2	60	81.35	81.71
1	30	60	2	2	60	80.15	80.82

A is initial Cr(VI) concentration (g/L), *B* is TSAC dose (g/100 mL), *C* is pH, and *D* is contact time (min).

The interaction effect of contact time and TSAC dose on removal efficiency of Cr(VI) is depicted in Figure 7(e). As it is illustrated through the 3D plots, it is clear that the removal of Cr(VI) by adsorption increases with the dosage of TSAC from 2 to 3 g/100 mL and declines with further increment. As contact time increased from 60 to 90 min, the adsorption efficiency also increased but become constant when contact time is more than 90 min. As predicted from the quadratic equation of response (equation (11)), the interaction effect of TSAC dose and contact time has a negative effect on the removal efficiency with a coefficient of -0.9119. The interaction effect has a significant effect on its Cr(VI) adsorption with a p value of 0.0117 (Table S2). The highest removal efficacy of Cr(VI) is attained at a TSAC dose of 3 g/100 mL and a contact time of 90 min.

Figure 7(f) demonstrates the interaction effect of the pH of the solution, and adsorption time on the adsorption of Cr(VI) via TSAC was substantial. The adsorption efficiency of TSAC was enlarged with an increment in contact time till the point of equilibrium is reached. It also keeps increasing with increments of adsorption time till it goes to 90 min and became constant with a further rise in adsorption time. As it is presented from the second-order polynomial equation (equation (11)), the interaction relations of TSAC dose and adsorption time have a negative effect on the TSAC removal competence with a coefficient of –1.21. It also has an important effect on the adsorption efficacy of TSAC with a p value of 0.0018 (Table S2). The peak for adsorption efficiency was attained at 2.5 pH and 90 min adsorption time.

3.3.3. Optimization of Selected Parameters for Cr(VI) Adsorption. Triplicate tests were executed to determine the significance of optimization outcome under optimal points projected by the CCD model. The observed (experimental) results of the removal efficacy of TSAC at those optimal levels were in close pact with the predicted value of the

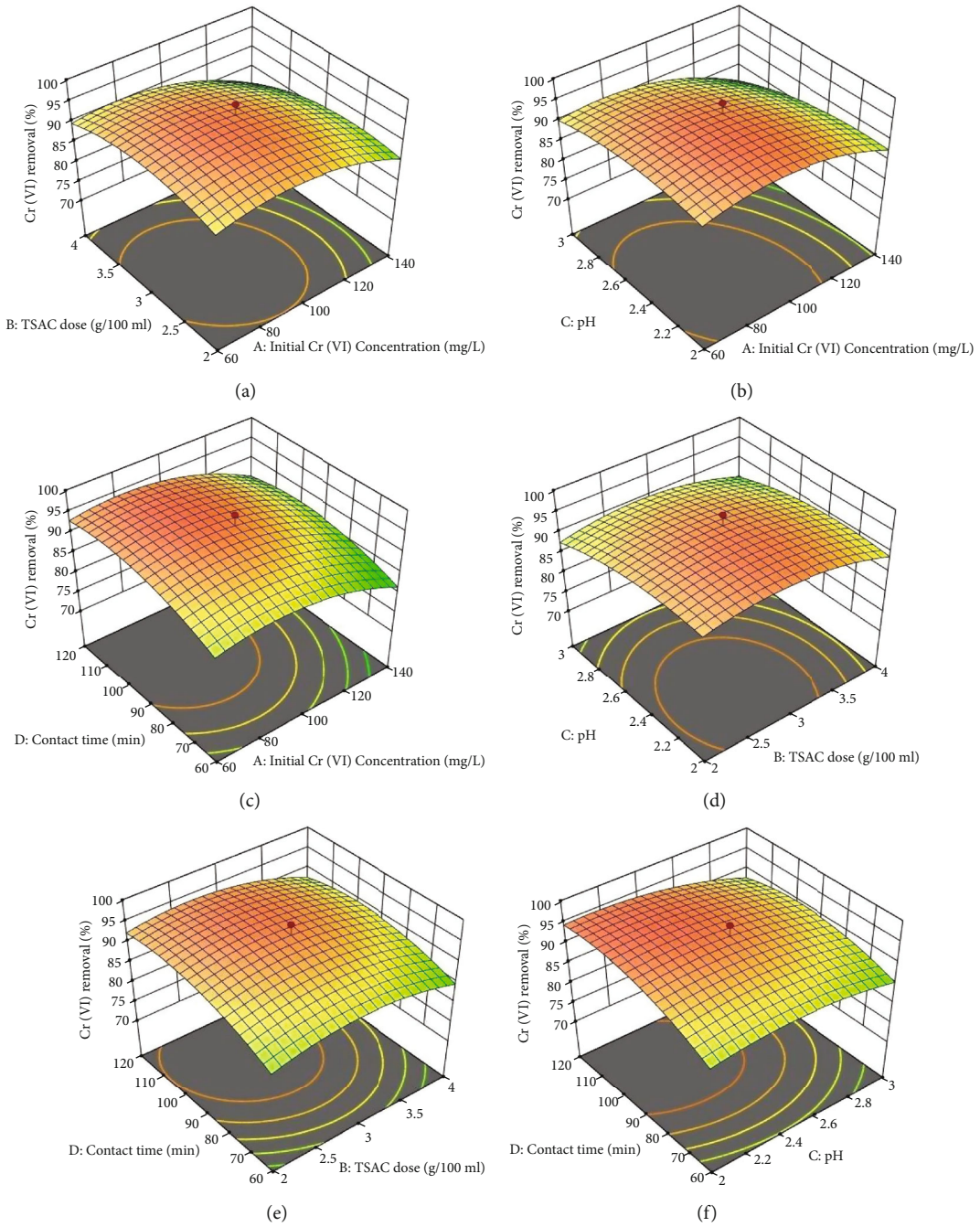

Figure 7: (a) Interaction effect of initial Cr(VI) concentration and TSAC dose, (b) initial Cr(VI) concentration and pH, (c) initial Cr(VI) concentration and contact time, (d) TSAC dose and pH, (e) TSAC dose and contact time, and (f) pH and contact time on Cr(VI) removal from aqueous media.

model (Table 6). Thus, this validation proves the suitability of the quadratic model for this process. In agreement with our data, Aravind et al. reported the effectiveness of gooseberry seed adsorbent-based activated carbon for the removal of Cr(VI) from the synthetic solution, and optimum adsorption of Cr(VI) (91.26% removal) is obtained at 60 mg/L of initial concentration of Cr(VI) and at 2 solution pH [43]. Almond shell-based AC showed 100% removal capacity of Cr(VI) form synthetic solution at a pH of 2 [45].

3.4. Adsorption Mechanism

3.4.1. Adsorption Isotherm Models. The well-known isotherm models, that is, Langmuir and Freundlich, were utilized in order to understand the adsorbate particle distribution between the adsorbent and the liquid, grounding on numerous assumptions which are mostly associated with the adsorbent homogeneity or heterogeneity, the type interaction possibility, and coverage among the particles of the adsorbate [13].

Table 6: Optimal conditions of the selected factors for Cr(VI) adsorption via TSAC.

Process parameters	Initial Cr(VI) concentration	TSAC dose	pH	Contact time	Removal efficiency (%)		Desirability
					Predicted	Actual	
Optimized conditions	87.57	2.742	2.2	109	96.161	95.90	0.984

The Langmuir model was founded on the postulation that the highest adsorption happens as soon as enough monolayer of solute particles exists on the adsorbent surface, keeping constant the adsorption energy, which means identical over all areas and there is not any migration of absorbable particles in the plane of the surface [46]. These are comparably better models of isotherm in explaining the adsorption of chemicals [46]. The Langmuir isotherm is given by the following equation:

$$\frac{C_e}{q_e} = \frac{1}{bq_{max}} + \frac{C_e}{q_{max}}. \quad (12)$$

The suitability of this can be examined through specific adsorption (C_e/q_e) versus the concentration of equilibrium (C_e) as the linear plot in Figure 8(a) (Table 7). The unknown value of constraints, namely, the adsorption energy (b) and the highest capacity of adsorption (q_{max}) can be measured from the intercept and slope of the plot given by equation (12) [47].

Freundlich isotherm can be employed to pronounce the adsorption process on a surface possessing the heterogeneous energy distribution. Freundlich isotherm is derived assuming heterogeneity surface and presented in a logarithmic scale using the expression. The suitability of the isotherm was verified via the equation (equation (13)) of the Freundlich model that is linearized:

$$\log q_e = \log K_f + \frac{1}{n} \log C_e, \quad (13)$$

where q_e denotes the quantity of adsorbed Cr(VI) per quantity of adsorbent at the conditions of equilibrium (mg/g), C_e denotes the equilibrium concentration (mg/L), K_f denotes the capacity of adsorption, and n denotes the intensity of adsorption. The value of Freundlich constants ($1/n$ and K_f) can be gotten through the $\ln(q_e)$ versus $\ln C_e$ plot (Figure 8(b)) (Table 7).

The outcomes given in Figure 8 discovered that a higher R^2 (0.996)was detected on the isothermal model of Langmuir. This indicates that Langmuir is more suitable to describe Cr(VI) adsorption via TSAC. From the result, it can be concluded that the active sites of TSAC were regularly dispersed and the monolayer adsorption via chemical adsorption is achieved.

3.4.2. Adsorption Kinetic Models. Kinetics of adsorption can be denoted as the rate of removal of solute that pedals the residence time of the sorbate in the interface of solution-solid. It is a great tool to investigate the effectiveness of a specified adsorbent and increase understanding of the fundamental mechanisms. The information gotten from the kinetic study has a significant role in selecting optimum conditions for larger-scale process design [51].

The residual concentration of hexavalent chromium, C_t was measured as per the time of function, and the uptake q_t was measured employing the following equation:

$$q_t = \frac{C_o - C_t}{W} V, \quad (14)$$

where C_t is the Cr(VI) concentration at any time t, q_t is the capacity of adsorption at any time; and V is the solution of Cr(VI) volume (mL). W (g) denotes of adsorbent utilized for the process of adsorption.

The model of pseudo-first-order kinetic adopts that the change in the degree of the solute adsorbed with time is directly proportionate to the change in the concentration at saturation point and the quantity of solid uptake through time. The suitability of this model was checked through the Lagergren model that is given by the following linearized equation [12]:

$$\log (q_e - q_t) = \log q_e - \frac{K_1}{2.303} t, \quad (15)$$

where q_e and q_t denote the quantity of adsorbed Cr(VI) (mg/g) at equilibrium condition and the quantity of adsorbed Cr(VI) (mg/g)at any instance of time t (min), respectively. K_1 denotes the rate constant which is deduced by pseudo-first-order kinetic (min^{-1}).The slope and intercept of the plot of log ($q_e q_t$) vs. t, respectively, may be used to calculate the values of K_1 and q_e. (Figure 9(a)), and they are summarized in Table 8.

The model of pseudo-second-order kinetic is grounded on the statement that the rate restraining phase may stem from the chemical adsorption concerning valence forces over the allocation or exchange of electrons among the adsorbate and adsorbent. The suitability of this kinetic model was verified with the given equation [13].

$$\frac{t}{q_t} = \frac{1}{K_2 q_e^2} + \frac{t}{q_e}, \quad (16)$$

where K_2 (g/mg·min) denotes the rate constant of the pseudo-second-order adsorption, q_t($mg\,g^{-1}$) is the amount of Cr(VI) on the surface of the adsorbent at any time t, and q_e ($mg\,g^{-1}$) is the quantity of Cr(VI) adsorbed at equilibrium. Values of q_e and K_2 can be evaluated from a linear plot of t/q_t versus t (Figure 9(b)), and they are given in Table 8.

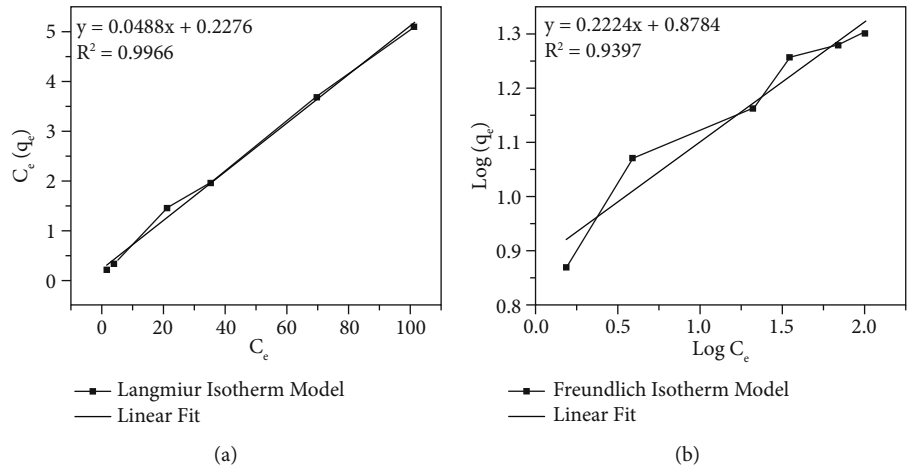

Figure 8: Isotherm model of (a) Langmuir model and (b) Freundlich model for removal of Cr(VI) via TSAC.

Table 7: Parameters obtained by Langmuir and Freundlich isotherms for Cr(VI) adsorption by TSAC.

Adsorbent	Langmuir			Freundlich			References
	q_{max}	b	R^2	K_f	n	R^2	
TSAC	20.49	0.2144	0.9966	7.558	4.464	0.9397	Present work
ACAP	36.01	—	0.9157	2.2637	1.570	0.99	[38]
LLAC	27.53	0.0681	0.9466	3.47	2.13	0.9798	[48]
Ch-based AC	20.04	0.05	0.877	1.02	1.204	0.863	[49]
BSAC	17.27	0.0848	0.9865	2.110	1.790	0.9996	[50]

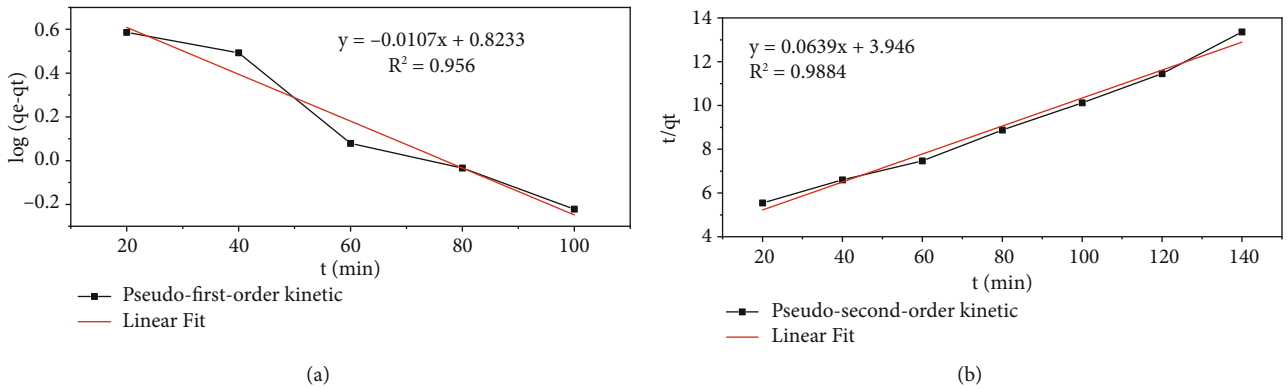

Figure 9: Fitting of adsorption data for (a) pseudo-first-order and (b) pseudo-second-order kinetic equations.

Findings that are presented in Figure 9 demonstrate that a higher value of R^2 (0.9884) was obtained for fitting of data with the pseudo-second-order kinetic model. This indicated that this model delivers the finest association of the data. Thus, the rate restraining step could be triggered by chemosorption linking valence forces over exchange of electrons among adsorbate and Cr(VI).

The validity of the intraparticle diffusion kinetic model was also tested by the magnitude of the regression coefficient. It showed that data was found to have poor fit to the adsorption data. Also, the kinetic data was analyzed using the intraparticle diffusion model. As seen in Figure 10, the plot did not pass through the origin which explicated that intraparticle diffusion was not the only rate-limiting step. The kinetic of Cr(VI) adsorption to the TSAC biosorbent was governed by the Elovich model. Using the linear plot of the Elovich model, the chemisorption rate (a_e) and surface coverage (b_e) constants were found to be 0.143 mg $(g{\cdot}min)^{-1}$ and 0.267 g$\cdot mg^{-1}$, respectively. From the results, it is clear that the heavy metal ions, Cr(VI), had lower value of adsorption rate by TSAC through chemisorption. However, the values may differ and depend with respect to the nature of activated carbon and processing condition. Further, the data were applied to examine the impact of pore diffusion on the adsorption process using the Bangham equation. The kinetic parameters and correlation coefficients

Table 8: The value of adsorption kinetic parameters and constants for removal of Cr(VI) by TSAC.

Kinetic model	Parameter	Value
Pseudofirst order	K_1	0.0246
	R^2	0.956
Pseudosecond order	K_2	0.00231
	R^2	0.9884
Intraparticle diffusion	k_w (mg·g^{-1}·min$^{-1/2}$)	0.9397
	C	0.4149
	R^2	0.8583
Elovich model	a_e (mg(g·min)$^{-1}$)	0.536
	b_e (g·mg^{-1})	0.267
	R^2	0.9365
Bangham's model	K_B (mL/g)	36.59
	A	-0.4021
	R^2	0.9313

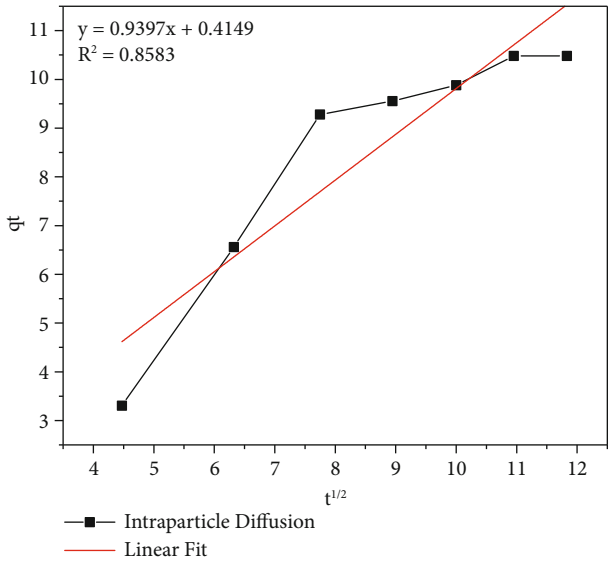

Figure 10: Intraparticle diffusion plot for removal of Cr(VI) by TSAC.

Table 9: Values of thermodynamic parameters for the biosorption of Cr(VI) using TSAC at different temperatures.

S. No	Temperature (°C)	Thermodynamic parameter ΔG (kJ/mol)	ΔH (kJ/mol)	ΔS (kJ/mol/K)
1	25	-1.334	27.54	91.26
2	40	-2.549		
3	60	-4.637		

are presented in Table 8 which were calculated using Bangham's equation. The explored data were observed to be fair in the fitting of the model (since $R^2 = 0.9313$). This

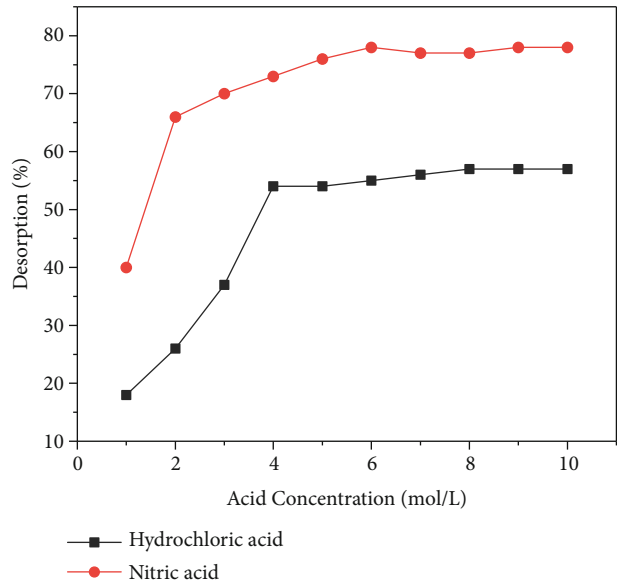

Figure 11: Desorption of Cr(VI) from TSAC with respect to different concentrations of hydrochloric acid and nitric acid.

inference indicated that the diffusion of TSAC adsorbate into pores of the sorbent is not the only rate-controlling step.

The outcomes of kinetics and isotherm investigations were consistent with previously studied data that were accomplished to investigate the kinetics of adsorption Cr(VI) in activated carbon prepared from agricultural wastes [27, 43, 52].

3.5. Thermodynamic Parameters. In this study, a plot of ln (K_d) *vs.* $[1/T]$ as shown in Figure 3 was generated. From the plot, the value of ΔS and ΔH was detected from the intercept and slope, respectively. The obtained values of thermodynamic parameters are presented in Table 9. From the results, change in enthalpy value was observed to be positive, which showed that the biosorption reaction is endothermic due to the increase in biosorption upon successive increase in the temperature. The negative value of ΔG revealed that the adsorption process by TSAC is thermodynamically spontaneous nature. The positive value of ΔS indicates enhanced randomization at the solid–solution interface during chromium ion biosorption on the active sites of the biosorbent.

3.6. Desorption and Regeneration of Adsorbent. Figure 11 depicts the desorption performance of the TSAC using HNO_3 and HCl. It was observed that the desorption was gradually increased with eluent concentration until a certain limit. This concentration was observed to be 4 mol/L for HCl and HNO_3. It was observed that the desorption cannot be significantly increased beyond this concentration limit. Even though both eluents showed almost the same pattern of desorption dynamics, HNO_3 showed a higher desorption efficiency than HCl. This investigation explicated that the maximum desorption of 78% of Cr(VI) was achieved using HNO_3 with 6 mol/L. It also confirmed that even the use of higher concentrated HCl or HNO_3 could not result in the

total desorption of heavy metal ions from the TSAC surface. In addition, it was clearly noticed that the adsorption process is reversible.

4. Conclusions

Eragrostis tef (teff) is an annual grass, a species to the Horn of Africa, notably to Ethiopia. The present study focused on the preparation of teff straw-based activated carbon (TSAC) and investigated its potential on adsorption of Cr(VI) from synthetic solution. The activated carbon was prepared using straw; further, it was characterized using different techniques such as BET, FTIR, SEM, and XRD. Adsorption experiments were carried out using prepared TSAC to optimize important independent parameters such as initial Cr(VI) concentration, dosage of TSAC, pH, and contact time using RSM. By adopting the design of experiments, statistically, it was optimized that the maximized removal (96.161%) of Cr(VI) can be achieved via TSAC at 87.57 mg/L, 2.742 g/100 mL, 2.22, and 109 min for initial Cr(VI) concentration, dosage of TSAC, pH, and contact time, respectively. From the kinetic studies, the high correlation coefficient Langmuir isotherm was found to be better fitted than Freundlich isotherm. The rate of Cr(VI) adsorption on the TASC was observed to fit better with the pseudo-second-order kinetic model with a good correlation coefficient. The thermodynamic parameters obtained show that the adsorption of the Cr(VI) on TASC is spontaneous and endothermic. In a nutshell, TSAC which was derived from locally obtainable agricultural wastes can be used as a potential adsorbent for Cr(VI) to remove the Cr(VI) from contaminated water.

Data Availability

The data used to support the findings of this study are included in the article.

Disclosure

This study was performed as a part of the Employment of School of Chemical Engineering, Jimma Institute of Technology, Jimma University, Jimma, Oromia, Ethiopia.

Conflicts of Interest

The authors declare that there are no conflicts of interest regarding the publication of this paper.

Acknowledgments

The authors thank Jimma Institute of Technology, Jimma University, Jimma, Oromia, Ethiopia, and Addis Ababa Science and Technology University, Addis Ababa, Ethiopia, for providing material and characterization supports to complete this research work.

Supplementary Materials

Table S1: ranges of selected process parameters at which adsorption experiments were conducted. Table S2: analysis of variance and second-order polynomial model coefficient of regression for adsorption of Cr(VI) from synthetic solution via TSAC. *(Supplementary Materials)*

References

[1] UNWWAP WWAP, *The United Nations World Water Development Report 2017. Wastewater: the untapped resource*, UNESCO, Paris, 2017, February 2021, https://unesdoc.unesco.org/ark:/48223/pf0000247153.

[2] P. S. Venkatesa, G. Girma, A. K. Gizachew, and B. M. Surafel, "Biosolubilization of Cr (VI) from tannery sludge: process modeling, optimization, rate kinetics and thermodynamics aspects," *International Journal of Recent Technology and Engineering*, vol. 8, pp. 4808–4816, 2019.

[3] B. Basaran, M. Ulas, B. O. Bitlisli, and A. Asian, "Distribution of Cr (III) and Cr (VI) in chrome tanned leather, Indian," *Journal of Chemical Technology & Biotechnology*, vol. 15, pp. 511–514, 2008.

[4] D. M. Proctor, M. Suh, S. L. Campleman, and C. M. Thompson, "Assessment of the mode of action for hexavalent chromium-induced lung cancer following inhalation exposures," *Toxicology*, vol. 325, pp. 160–179, 2014.

[5] Black Smith Institute Report, *The world's worst polluted places*, 2015, https://www.worstpolluted.org/docs/WWP15.pdf.

[6] P. Amoatey and M. S. Baawain, "Effects of pollution on freshwater aquatic organisms," *Water Environment Research*, vol. 91, no. 10, pp. 1272–1287, 2019.

[7] J. Grumiller and W. Raza, *The Ethiopian Leather and Leather Products Sector: An Assessment of Export Potentials to Europe and Austria*, 2019.

[8] B. Volesky, "Detoxification of metal-bearing effluents: biosorption for the next century," *Hydrometallurgy*, vol. 59, no. 2-3, pp. 203–216, 2001.

[9] Y. Wang, H. Su, Y. Gu, X. Song, and J. Zhao, "Carcinogenicity of chromium and chemoprevention: a brief update," *Oncotargets and Therapy*, vol. 10, pp. 4065–4079, 2017.

[10] D. Berihun, "Removal of chromium from industrial wastewater by adsorption using coffee husk," *Journal of Materials Science and Engineering*, vol. 6, no. 2, pp. 6–11, 2017.

[11] F. Kebede and G. Alemayehu, "Removal of chromium and azo metal-complex dyes using activated carbon synthesized from tannery Wastes," *Journal of Science and Technology*, vol. 5, no. 2, pp. 1–30, 2017.

[12] S. M. Beyan, S. V. Prabhu, T. T. Sissay, and A. A. Getahun, "Sugarcane bagasse based activated carbon preparation and its adsorption efficacy on removal of BOD and COD from textile effluents: RSM based modeling, optimization and kinetic aspects," *Bioresource Technology Reports*, vol. 14, article 100664, 2021.

[13] Y. Asrat, A. T. Adugna, M. Kamaraj, and S. M. Beyan, "Adsorption phenomenon of Arundinaria alpina stem-based activated carbon for the removal of lead from aqueous solution," *Journal of Chemistry*, vol. 2021, Article ID 5554353, 9 pages, 2021.

[14] T. A. Amibo, S. M. Beyan, and T. M. Damite, "Novel lanthanum doped magnetic teff straw biochar nanocomposite and

optimization its efficacy of defluoridation of groundwater using RSM: a case study of Hawassa city, Ethiopia," *Advances in Materials Science and Engineering*, vol. 2021, Article ID 9444577, 15 pages, 2021.

[15] E. Meez, A. Rahdar, and G. Z. Kyzas, "Sawdust for the removal of heavy metals from water: a review," *Molecules*, vol. 26, p. 4318, 2021.

[16] M. Czikkely, E. Neubauer, I. Fekete, P. Ymeri, and C. Fogarassy, "Review of heavy metal adsorption processes by several organic matters from wastewaters," *Watermark*, vol. 10, p. 1377, 2018.

[17] W. Kidus Tekleab, S. M. Beyan, S. Balakrishnan, and H. Admassu, "Chicken feathers based keratin extraction process data analysis using response surface-box-Behnken design method and characterization of keratin product," *Current Applied Science and Technology*, vol. 20, pp. 163–177, 2020.

[18] ASTM, "D2495-07, standard test method for moisture in cotton by oven-drying," *ASTM Int.*, 2019.

[19] ASTM, "D2866-11, standard test method for Total ash content of activated carbon," *ASTM Int.*, 2018.

[20] ASTM, "D5832-98, standard test method for volatile matter content of activated carbon samples," *ASTM Int.*, 2014.

[21] ASTM, "D2854-09, standard test method for apparent density of activated carbon," *ASTM Int.*, 2019.

[22] ASTM, "D7582-15, standard test methods for proximate analysis of coal and coke by macro thermogravimetric analysis," *ASTM Int.*, 2015.

[23] T. Mkungunugwa, S. Manhokwe, A. Chawafambira, and M. Shumba, "Synthesis and characterisation of activated carbon obtained from Marula (Sclerocarya birrea) nutshell," *Journal of Chemistry*, vol. 2021, Article ID 5552224, 9 pages, 2021.

[24] S. Kodama and H. Sekiguchi, "Estimation of point of zero charge for activated carbon treated with atmospheric pressure non-thermal oxygen plasmas," *Thin Solid Films*, vol. 506–507, pp. 327–330, 2006.

[25] ASTM, "E70-19, standard test method for pH of aqueous solutions with the glass electrode," *ASTM Int.*, 2019.

[26] M. K. Rai, G. Shahi, V. Meena et al., "Removal of hexavalent chromium Cr (VI) using activated carbon prepared from mango kernel activated with H3PO4," *Resource-Efficient Technologies*, vol. 2, pp. S63–S70, 2016.

[27] T. Dula, K. Siraj, and S. A. Kitte, "Adsorption of hexavalent chromium from aqueous solution using chemically activated carbon prepared from locally available waste of bamboo (Oxytenanthera abyssinica)," *ISRN Environmental Chemistry*, vol. 2014, Article ID 438245, 9 pages, 2014.

[28] P. K. Ghosh, "Hexavalent chromium [Cr(VI)] removal by acid modified waste activated carbons," *Journal of Hazardous Materials*, vol. 171, pp. 116–122, 2009.

[29] S. I. Mussatto, M. Fernandes, G. J. M. Rocha, J. J. M. Órfão, J. A. Teixeira, and I. C. Roberto, "Production, characterization and application of activated carbon from brewer's spent grain lignin," *Bioresource Technology*, vol. 101, pp. 2450–2457, 2010.

[30] P. Senthil Kumar, G. J. Joshiba, C. C. Femina et al., "A critical review on recent developments in the low-cost adsorption of dyes from wastewater, Desalin," *Desalination and Water Treatment*, vol. 172, pp. 395–416, 2019.

[31] D. Mihayo, M. R. Vegi, and S. A. H. Vuai, "Defluoridation of aqueous solution using thermally activated biosorbents prepared from Adansonia digitata fruit pericarp," *Adsorption Science and Technology*, vol. 2021, article 5574900, 16 pages, 2021.

[32] S. M. Beyan, T. A. Amibo, S. V. Prabhu, and A. G. Ayalew, "Production of nanocellulose crystal derived from enset fiber using acid hydrolysis coupled with ultrasonication, isolation, statistical modeling, optimization, and characterizations," *Journal of Nanomaterials*, vol. 2021, Article ID 7492532, 12 pages, 2021.

[33] T. K. Mumecha, B. Surafel Mustefa, S. Venkatesa Prabhu, and F. T. Zewde, "Alkaline protease production using eggshells and membrane-based substrates: process modeling, optimization, and evaluation of detergent potency," *Engineering and Applied Science Research*, vol. 48, pp. 171–180, 2021.

[34] L. Zhou, Y. Liu, S. Liu et al., "Investigation of the adsorption-reduction mechanisms of hexavalent chromium by ramie biochars of different pyrolytic temperatures," *Bioresource Technology*, vol. 218, pp. 351–359, 2016.

[35] Wang, Zhang, and Lv, "Removal efficiency and mechanism of Cr(VI) from aqueous solution by maize straw biochars derived at different pyrolysis temperatures," *Watermark*, vol. 11, no. 4, p. 781, 2019.

[36] X. Zhang, W. Fu, Y. Yin et al., "Adsorption-reduction removal of Cr(VI) by tobacco petiole pyrolytic biochar: batch experiment, kinetic and mechanism studies," *Bioresource Technology*, vol. 268, pp. 149–157, 2018.

[37] M. W. Rahman, M. Y. Ali, I. Saha et al., "Date palm fiber as a potential low-cost adsorbent to uptake chromium (VI) from industrial wastewater, Desalin," *Desalination and Water Treatment*, vol. 88, pp. 169–178, 2017.

[38] I. Enniya, L. Rghioui, and A. Jourani, "Adsorption of hexavalent chromium in aqueous solution on activated carbon prepared from apple peels," *Sustainable Chemistry and Pharmacy*, vol. 7, pp. 9–16, 2018.

[39] Ş. Parlayici and E. Pehlivan, "Comparative study of Cr(VI) removal by bio-waste adsorbents: equilibrium, kinetics, and thermodynamic," *Journal of Analytical Science and Technology*, vol. 10, pp. 1–8, 2019.

[40] D. Mohan, K. P. Singh, and V. K. Singh, "Removal of hexavalent chromium from aqueous solution using low-cost activated carbons derived from agricultural waste materials and activated carbon fabric cloth," *Industrial and Engineering Chemistry Research*, vol. 44, pp. 1027–1042, 2005.

[41] Z. A. AL-Othman and M. N. Ali, "Hexavalent chromium removal from aqueous medium by activated carbon prepared from peanut shell: adsorption kinetics, equilibrium and thermodynamic studies," *Chemical Engineering Journal*, vol. 184, pp. 238–247, 2012.

[42] N. Gnanasundaram, M. Loganathan, and A. Singh, "Optimization and performance parameters for adsorption of Cr 6+ by microwave assisted carbon from Sterculia foetida shells," *IOP Conference Series: Materials Science and Engineering*, vol. 206, article 012065, 2017.

[43] J. Aravind, P. Kanmani, G. Sudha, and R. Balan, "Optimization of chromium (VI) biosorption using gooseberry seeds by response surface methodology," *Global Journal of Environmental Science and Management*, vol. 2, pp. 61–68, 2016.

[44] S. Mustefa Beyan, S. Venkatesa Prabhu, T. K. Mumecha, and M. T. Gemeda, "Production of alkaline proteases using aspergillus sp. isolated from Injera: RSM-GA based process optimization and enzyme kinetics aspect," *Current Microbiology*, vol. 78, pp. 1823–1834, 2021.

[45] M. K. Rai, B. S. Giri, Y. Nath et al., "Adsorption of hexavalent chromium from aqueous solution by activated carbon prepared from almond shell: kinetics, equilibrium and thermodynamics study," *Journal of Water Supply: Research and Technology-AQUA*, vol. 67, pp. 724–737, 2018.

[46] L. Liu, Y. Rao, C. Tian et al., "Adsorption Performance of La(III) and Y(III) on Orange Peel: Impact of Experimental Variables, Isotherms, and Kinetics," *Adsorption Science and Technology*, vol. 2021, article 7189639, 12 pages, 2021.

[47] A. Q. Alorabi, "Effective removal of malachite green from aqueous solutions using magnetic nanocomposite: synthesis, characterization, and equilibrium study," *Adsorption Science and Technology*, vol. 2021, article 2359110, 15 pages, 2021.

[48] A. S. Yusuff, "Optimization of adsorption of Cr(VI) from aqueous solution by Leucaena leucocephala seed shell activated carbon using design of experiment," *Applied Water Science*, vol. 8, pp. 1–11, 2018.

[49] F. H. Emamy, A. Bumajdad, and J. P. Lukaszewicz, "Adsorption of hexavalent chromium and divalent lead ions on the nitrogen-enriched chitosan-based activated carbon," *Nanomaterials*, vol. 11, 2021.

[50] J. Anandkumar and B. Mandal, "Removal of Cr(VI) from aqueous solution using Bael fruit (Aegle marmelos correa) shell as an adsorbent," *Journal of Hazardous Materials*, vol. 168, pp. 633–640, 2009.

[51] S. Venkatesa Prabhu, G. Ramesh, A. T. Adugna, S. M. Beyan, and K. Gizachew Assefa, "Kinetics of iron bioleaching using isolated Leptospirillum ferriphilum: effect of temperature," *International Journal of Innovative Technology and Exploring Engineering*, vol. 8, pp. 76–81, 2019.

[52] E. Pantazopoulou, O. Zebiliadou, M. Mitrakas, and A. Zouboulis, "Stabilization of tannery sludge by co-treatment with aluminum anodizing sludge and phytotoxicity of end-products," *Waste Management*, vol. 61, pp. 327–336, 2017.